DMD Fast Forward. Published on October 6, 2008 as doi:10.1124/dmd.108.024174
This article has not been copyedited and formatted. The final version may differ from this version.

DMD#24174

Circadian Expression Profiles of Drug Processing Genes and Transcription Factors in Mouse Liver[i]

Yu-Kun Jennifer Zhang, Ronnie L. Yeager and Curtis D. Klaassen[1]

Department of Pharmacology, Toxicology and Therapeutics,

University of Kansas Medical Center,

Kansas City, KS 66160

DMD Fast Forward. Published on October 6, 2008 as DOI: 10.1124/dmd.108.024174
This article has not been copyedited and formatted. The final version may differ from this version.

Running Title**:** Circadian rhythm of hepatic drug-metabolizing genes

[1] Author whom to address correspondence: Curtis D. Klaassen, PhD., Department of Pharmacology, Toxicology and Therapeutics, University of Kansas Medical Center, Kansas City, KS 66160. Email: cklaasse@kumc.edu, Phone: 913-588-7500, Fax 913-588-7501.

Text Pages: 34
Reference: 35
Figures: 13
Abstract Words 216
Introduction Words 730
Discussion Words 1395

Abbreviations: AhR, aryl hydrocarbon receptor; Alas1, Delta-aminolevulinic acid synthase; Aldh, aldehyde dehydrogenase; Arnt, aryl hydrocarbon receptor nuclear translocator; Atp8b1, ATPase, class I, type 8b, member 1; Bcrp, breast cancer resistance protein; Bmal1, brain and muscle Arnt-like protein 1; Bsep, bile salt export pump; CAR, constitutive androstane receptor; C/EBP, CAAT/enhancer-binding protein; Ces, carboxylesterase; Cpr, Cytochrome P450 reductase; Cyp, cytochrome P450 enzymes; Dbp, albumin D site binding protein; DPG, drug processing gene; Gst, glutathione *S*-transferase; HNF, hepatocyte nuclear factor; Keap1, Kelch-like ECH-associated protein 1; Mate1, multidrug and toxin extrusion 1; Mdr, multidrug resistance; Mrp, multidrug resistance-associated protein; Nqo, NAD(P)H:quinone oxidoreductase; Nrf2, nuclear factor erythoroid 2 related factor 2; Ntcp, sodium taurocholate cotransporting polypeptide; Oat, organic anion transporter; Oatp, organic anion transporting polypeptide; Oct, organic cation transporter; PAPS, phosphoadenosine-5'-

phosphosulfate; Papss2, PAPS synthase 2; Pon, paraoxonase; PPARα, peroxisomal proliferator activated receptor alpha; PXR, pregnane X receptor; Sult, sulfotransferase; UDP-GA, UDP-glucuronic acid; Ugt, UDP-glucuronosyltransferase.

Abstract

Temporal coordination of hepatic drug processing gene (DPG) expression facilitates absorption, biotransformation, and excretion of exogenous and endogenous compounds. To further elucidate the circadian rhythm of hepatic DPG expression, male C57BL/6 mice were subjected to a standard 12-h light/dark cycle and livers were collected at 0200, 0600, 1000, 1400, 1800, and 2200. The mRNAs of hepatic phase-I enzymes (Cyps, Aldhs, and Cess), phase-II enzymes (Ugts, Sults, and Gsts), uptake and efflux transporters, as well as transcription factors were quantified. Messenger RNAs of various genes were graphed across time of day and compared by hierarchical clustering. In general, the mRNA of phase-I enzymes increased during the dark phase, whereas mRNA of most phase-II enzymes and transporters reached maximal levels during the light phase. The majority of hepatic transcription factors exhibited expression peaks either prior to or after the onset of the dark phase. During the same time period, the negative clock regulator gene Rev-Erbα and the hepatic clock-controlled gene Dbp also reached mRNA expression peaks. Considering their important role in xenobiotic metabolism, hepatic transcription factors, such as CAR, PXR, AhR, and PPARα, may be involved in coupling the hepatic circadian clock to environmental cues. Collectively, these data demonstrate the circadian expression of the DPG battery and transcription factors contributes to the temporal detoxification cycle in the liver.

Introduction

The mammalian circadian system temporally coordinates proliferation and metabolism in the body. Disrupting the circadian rhythm, as observed in rotating shift workers, has been reported to lead to an increased incidence of breast and colon cancer (Haus and Smolensky, 2006). Xenobiotic detoxification systems in liver, intestine, and kidney, among many other metabolic processes, are subjected to the hierarchical coordination by the central clock in the suprachiasmatic nucleus and the peripheral clock in each organ (Levi and Schibler, 2007). Optimizing drug dosing time has been suggested to be an important consideration for the treatment of several chronic diseases and cancer.

Liver is the major tissue for drug metabolism and contains most of the drug processing genes (DPGs) in the body. Hepatic DPGs include genes encoding phase-I and -II metabolizing enzymes, as well as uptake and efflux transporters.

Hepatobiliary transporters play important roles in uptake and clearance of xenobiotics by the liver, contributing to the “first-pass effect”. The hepatic solute carrier family of proteins mediate uptake of xenobiotics across the sinusoidal membrane. These transporters include Na^+-taurocholate cotransporting polypeptide (Ntcp); organic anion transporting polypeptide 1a1 (Oatp1a1), 1a4, 1b2, 2b1; organic anion transporter 2 (Oat2); organic cation transporter 1 (Oct1); and equilibrative nucleoside transporter 1 (Klaassen and Lu, 2008). Xenobiotics or their metabolites are transported out of hepatocytes into bile by canalicular transporters including multidrug resistance-associated protein 2 (Mrp2), breast

cancer resistance protein (Bcrp), multidrug resistance protein 1 (Mdr1), mutidrug and toxin extrusion 1 (Mate1), as well as the bile salt export pump (Bsep). Another excretory route of liver is transporting xenobiotics and their metabolites back into the blood to be eliminated by kidneys into urine. Transporters Mrp3, 4, and 6, situated on the sinusoidal membrane of hepatocytes, are responsible for this “alternative efflux” process. On the canalicular membrane of hepatocytes and cholangiocytes, the flippase Atpase 8b1 (Atp8b1) translocates aminophospholipids from the outer to inner leaflet, whereas Mdr2 translocates phosphatidylcholine from the inner to outer leaflet.

Xenobiotic metabolism within hepatocytes consists of two major divisions. Phase-I enzymes, including cytochrome P450s (Cyps), alcohol dehydrogenases (Adhs), aldehyde dehydrogenases (Aldhs), carboxylesterases (Cess), epoxide hydrolases, NAD(P)H:quinone oxidoreductases (Nqos), and paraoxonases (Pons), carry out oxidation, reduction, and hydrolysis reactions on substrates to introduce or unmask functional groups (Parkinson and Ogilvie, 2008). Metabolites of phase-I reactions are more water-soluble. In many cases, functional groups produced by phase-I metabolism are further conjugated with glucuronic acid, sulfate, glutathione, or amino acids, catalyzed by phase-II enzymes UDP-glucuronosyltransferases (Ugts), sulfotransferases (Sults), glutathione *S*-transferases (Gsts), and *N*-acetyltransferases, respectively. Generally, conjugation reactions markedly increase the hydrophilicity of xenobiotics and enhance their excretion into bile and/or blood.

DMD Fast Forward. Published on October 6, 2008 as DOI: 10.1124/dmd.108.024174
This article has not been copyedited and formatted. The final version may differ from this version.

Hepatic transcription factors play crucial roles in regulating the expression of DPGs. Upon activation, transcription factors release co-repressors and recruit co-activators, and initiate target gene expression by binding to specific response elements within regulatory regions. Nuclear receptors, such as constitutive androstane receptor (CAR), pregnane X receptor (PXR), peroxisomal proliferator-activated receptor alpha (PPARα), hepatocyte nuclear factor 4α (HNF4α), as well as other transcription factors, including aryl hydrocarbon receptor (AhR), nuclear factor erythroid 2 related factor 2 (Nrf2), HNF1α, and CAAT/enhancer-binding proteins (C/EBPs), are key mediators in coordinating DPG expression. Moreover, CAR, PXR, and AhR are recognized as xenobiotic sensors. They regulate a battery of phase-I and -II enzymes, as well as membrane transporters to accelerate the elimination of toxicants (Klaassen and Slitt, 2005; Nakata et al., 2006).

Diurnal rhythms in catalyzing activity of rodent hepatic enzymes have been known for decades. For example, circadian rhythms were demonstrated in the metabolism of aminopyrine and *p*-nitroanisole in male rats and mice in the 1960's (Radzialowski and Bousquet, 1968). The profound effect of the circadian clock on drug metabolism was highlighted recently in mice with mutations in three circadian-controlled PARbZip transcription factors, including albumin D site binding protein (Dbp). These triple-mutant mice have increased sensitivity to xenobiotics and premature aging (Gachon et al., 2006). Thus, the circadian oscillator, consisting of the core circadian transcription factors Clock, Bmal1, Rev-Erbα, Periods, and Cryptochromes, together with circadian-controlled genes,

such as the PARbZip transcription factors, adds another dimension to xenobiotic metabolism. However, less is known about the overall circadian expression of hepatic DPGs and the underlying regulatory mechanisms. Thus, the present study characterized the daily expression patterns of phase-I and -II drug-metabolizing enzymes, uptake and efflux transporters, hepatic transcription factors, as well as representative circadian transcription factors in mouse liver, in an attempt to reveal their potential inter-relationships**.**

Experimental Procedures

Animals. Animal experiments were performed in accordance with the institutional animal care and use committee guidelines. Male C57BL/6 mice (7 weeks of age) were purchased from Charles River and acclimated for 2 weeks in a temperature/humidity controlled facility with a standard 12-h light schedule (lights on at 0500 and off at 1700). All animals were given *ad libitum* access to water and standard rodent chow (Harlan Teklad #8604). Mice (n=5 per time point) were anesthetized within 20 min before 0200, 0600, 1000, 1400, 1800, and 2200. Livers were collected, rinsed with ice-cold saline, frozen in liquid nitrogen, and stored at -80°C.

Multiplex Suspension Array. Total RNA was extracted from livers using RNABee reagent (Tel-Test Inc., Friendswood, TX) according to the manufacturer's protocol, and was quantified spectrophotometrically. Equal amounts of RNA from individual samples were combined to make a pooled sample for each time point. The mRNA expression of genes of interest in livers was determined by Panomics 1.0/2.0 Quantigene plex technology (Panomics Inc., Fremont, CA). Panels were designed by Panomics and individual gene information can be found in the following plex sets on Panomics website (www.panomics.com): 20021, 2051, 2053, 2055, 2058, and 2061. Briefly, in a 96-well plate, 10 µg pooled RNA sample (n=5 per time point) was added to wells containing X-MAP beads coated with capture probes, label extenders, and blockers. The plate was incubated overnight at 54ºC. Beads and bound target mRNA were then transferred to filter plates, washed 3 times, and incubated with

amplifier at 46°C for 1 h. Wells were then washed twice and incubated with label (biotin) at 46°C for 1 h, washed again twice and incubated with Streptavidin-conjugated R-Phycoerythrin (SAPE), which binds biotinylated probes, and incubated at room temperature for 30 min. SAPE fluorescence was analyzed using a Bio-Plex 200 system array reader with Luminex 100 X-MAP technology, and data were acquired using Bio-Plex data manager software 4.1 (Bio-Rad, Hercules, CA). Messenger RNA expression is presented as relative light units (RLUs) per 10 µg of total RNA. In all graphs of this study, peak stands for the highest gene expression level and trough is the lowest during a 24-h period.

bDNA Assay. To verify the circadian expression patterns of genes displaying strong or weak signals in multiplex suspension assay, branched DNA (bDNA) signal amplification assay (Quantigene High Volume bDNA Signal Amplification Kit, Panomics Inc., Fremont, CA) was carried out for individual genes. For highly expressed genes (Cyp2e1, Cyp3a11, Ces5b1, and Pon1), 1 µg of total RNA was added per well. For lowly expressed genes (Cyp2b10, Mdr1, Kelch-like ECH-associated protein 1 [Keap1], and AhR), 10 µg RNA was loaded per well. Probe sets for these genes were previously published (Cheng et al., 2005b; Cheng and Klaassen, 2006; Petrick and Klaassen, 2007), and the bDNA procedure was carried out as described previously (Hartley and Klaassen, 2000). Briefly, pooled RNA was added to each well of a 96-well plate containing premixed capture hybridization buffer (50 µl) and diluted probe set (50 µl). Overnight hybridization between RNA and probe sets was performed at 53°C. Subsequent hybridization and post-hybridization wash steps were carried out according to the

manufacturer's protocol, and luminescence was quantified with Synergy 2 Multi-Detection Microplate Reader interfaced with Gen5 Reader Control and Data Analysis Software (Biotek, Winoosky, VT).

Expression Profiles by Hierarchical Clustering. For each gene, mRNA expression at each time point (0200, 0600, 1000, 1400, 1800, and 2200) was expressed as the ratio of expression at 0600. Patterns of gene expression across time were distinguished by hierarchical clustering (jmp V.7, SAS Institute, Cary, N.C.). Peak expression for each gene is represented by the darkest region of the gray-scale spectrum, with lowest expression indicated by the lightest (gray) region. Each spectrum is specific to the scale of mRNA expression for each gene on an individual basis. Therefore, the relative intensities of gray-scale spectra cannot be compared between genes.

Results

Diurnal expression of circadian transcription factors in the liver. As expected, components of the circadian clock displayed the most marked oscillations (Fig. 1). In this manuscript, peak stands for the highest expression level and trough is the lowest during the 24-h period. Messenger RNA of the core circadian transcription factor, Bmal1, was robust between 0200 and 1000 and only about 4.3% of the maximal level between 1400 and 1800. Rev-Erbα, the important negative clock regulator, oscillated in anti-phase to Bmal1. Rev-Erbα mRNA at 1400 was about 110-fold higher than at 2200 and 0600. The important hepatic clock-controlled gene Dbp, another liver-enriched transcription factor, was also expressed anti-phase to Bmal1. Similar to Rev-Erbα, the mRNA of Dbp was markedly increased at 1400 and by 1800 reached a peak that was 68.7-fold higher than at 0200 and 0600.

***Diurnal expression profiles of hepatic uptake transporters*.** The transcripts of Oatps tended to be more abundant during the light than the dark phase. As shown in Fig. 2, liver-enriched Oatp1a1, 1a4, and the liver-specific Oatp1b2 (Cheng et al., 2005a), uniformly peaked around 1400 with peak/trough ratio varying from 1.7 to 2.3. Oatp2b1 mRNA had a minimal fluctuation over 24-h in mouse livers. The mRNA of Oat2 was higher between 1000 and 1800, with a 1.6-fold peak/trough ratio. Similar to hepatic Oatps, the electrogenic uniporter Oct1 exhibited a single 60% increase of mRNA at 1400 and remained consistently low during the dark phase. No significant daily fluctuations were

observed in expression of the bile acid transporter Ntcp, nor the bi-directional nucleoside transporter equilibrative nucleoside transporter 1 (data not shown).

Daily variation in the expression of phase-I enzymes. The mRNA of major microsomal Cyps tended to accumulate more in the dark phase. As shown in Fig. 3, Cyp2b10 mRNA displayed a robust circadian rhythm with a peak/trough ratio of 2.8; the highest expression occurred at 0200 and the lowest at 1400. Cyp2e1 and Cyp3a11 demonstrated highest mRNA levels at 2200 and 0200, with peak/trough ratios of 1.6 and 1.8, respectively. Cyp4a14 mRNA exhibited marked fluctuation with a 5-fold peak/trough ratio during the dark phase. Whereas Cyp4a14 expression was relatively consistent during the light phase, its mRNA reached the highest expression at 1800, then rapidly declined to the lowest level in the middle of the dark phase (2200-0200), and returned to a higher level in the light-phase. The daily change in Cyp1a2 mRNA is 1.3-fold, with the peak at 1800 (data not shown). Cytochrome P450 reductase (Cpr), the common electron donor for Cyps, presented a marked circadian fluctuation of mRNA with a 3.8-fold peak/trough ratio. The Cpr mRNA was robustly expressed at 1800 and 2200, and remained at a low level during the day. The active site of cytochrome P450 contains a heme iron center. Delta-aminolevulinic acid synthase (Alas1) is the rate-limiting enzyme in the synthesis of heme. Messenger RNA of Alas1 oscillated with a 7.8-fold magnitude, and peaked at 1800.

The Aldh enzyme family carries out a diversity of metabolic functions, including detoxification. This study quantified mRNA of Aldh1a1, 1b1, 2, 3a2,

4a1, 6a1, 7a1, 8a1, and 9a1in mouse liver. Generally, the Aldh mRNAs tended to be higher in the dark phase, but the variations were less than 1.5 fold. The circadian expression patterns of Aldh1a1, 1a7, 2, and 3a2 are shown in Fig. 4 as representatives, whereas the other Aldhs are not shown. Aldh1a1 and 3a2 peaked at 1800. Aldh1a7 displayed the highest fluctuation among the Aldhs, with a peak (peak/trough ratio 1.9) at 0200. Aldh2 mRNA was equally expressed during the 24-h cycle.

Hepatic Ces isoenzymes hydrolyze ester- and amide-containing compounds. Fig. 5 illustrates typical circadian variations of Ces mRNAs, namely Ces1b4 (also known as Esd), 1d1, 1e1, 2a6, 5b1, and 6. Expression profiles of Ces1g2, 1h1, and 3a2 were not shown because of small daily variations; peak/trough values were 1.1, 1.2, and 1.4, respectively. Similar to the Aldhs, the majority of the Ces transcripts displayed mild fluctuations in mRNA over time, with slightly higher levels during the dark. The peak/trough ratio ranged from 1.1 (Ces1g2 and 5b1) to 1.6 (Ces1e1 and 2a6). Interestingly, many Ces mRNAs, including Ces1d1, 1e1, 2a6, 5b1, and 6, exhibited an additional minor trough in the middle of the dark phase (2200).

Paraoxonases (Pon) hydrolyze a broad range of organophosphorus esters. Pon1 and Pon3 are the two isoforms highly expressed in mouse liver. Both Pons were evenly expressed during the light phase. However, their expression profiles were divergent during the dark phase. Pon1 exhibited approximately a 40% decrease in mRNA at 2200 and 0200, whereas Pon3 mRNA increased 40% at 0200 (Fig. 6). Fig. 6 also shows the flat daily expression pattern of the cytosolic

flavoprotein Nqo1, which catalyzes the reduction of quinones and protects against oxidative stress.

***Daily variation in the expression of phase-II enzymes*.** The circadian expression patterns of major hepatic UGTs are shown in Fig. 7. Ugt1a1, 1a6, and 1a9 exhibited slightly higher mRNA expression in the late-light phase (peak/trough values between 1.3 and 1.5; represented by Ugt1a1 in Fig. 7), whereas Ugt1a5 is different from the other Ugt1a mRNAs by displaying a brief 1.8-fold mRNA peak at 0200. The hepatic specific Ugt2b1 exhibited slightly higher (30%) mRNA expression around the light/dark transitions (0600 and 1800). Similar to most of the Ugt1a mRNAs, several Ugt2 family members also exhibited highest mRNA expression in the late-light phase (1400), including Ugt2a3 (1.8 fold), Ugt2b35 (1.6 fold, not shown), and Ugt2b36 (1.9 fold). In contrast to other Ugts, Ugt2b34 displayed a unique circadian pattern, with the highest mRNA level at 0600 and lowest at 1800. In mouse liver, Ugt3a1 and 3a2 were expressed slightly higher in the light phase (peak/trough values of 1.4 and 1.3, respectively, data not shown). The two enzymes involved in the biosynthesis of UDP-glucuronic acid (UDP-GA), the co-substrate for glucuronidation, exhibited different circadian expression patterns. The mRNA of UDPG-pyrophosphorylase (UDP-gpp), the enzyme that catalyzes the formation of UDP-glucose from glucose-1-phosphate and UTP, exhibited abundant circadian rhythmicity, with a 2.4-fold peak at 1400. However, UDPG-dehydrogenase (UDP-gdh), the enzyme that subsequently oxidizes UDP-glucose to UDP-GA, only exhibited a 1.3-fold variation in mRNA.

Among the 7 hepatic Sult isoforms quantified in livers of male mice, Sult1a1 and 1d1 exhibited high-level mRNA expression, Sult5a1 was moderate, whereas mRNAs of Sult1c1, 1e1, 2a2, and 3a1 were not detected. mRNA levels of Sult1a1, 1d1, and 5a1 oscillated with 1.5-, 3.0-, and 2.4-fold amplitudes, respectively, with peaks appearing around the day to night transition (Fig. 8). 3'-phosphoadenosine-5'-phosphosulfate (PAPS) provides sulfonate groups for sulfo-conjugation catalyzed by all Sults. PAPS synthase 2 (Papss2) is the rate-limiting enzyme for the production of PAPS in liver. PAPSs2 mRNA reached peak levels at 1800, and remained elevated until 0200, and then decreased to a trough at 0600 (peak/trough ratio 2.6).

Many isoforms of Gsts are abundantly expressed in liver. Gsta1/2 (2.8 fold) and Gsta4 (2.4 fold) transcripts exhibited the largest daily fluctuations (Fig. 9); both displaying highest expression in the early-light phase (1000) and lowest in the middle-dark phase (around 2200). Circadian rhythms of the five mu family Gsts are similar to those of the two alpha Gsts. Gstm2, exhibiting a 2.1-fold daily fluctuation in mRNA expression, is shown in Fig. 9, whereas circadian variations of Gstm1, m3, m4, and m6, with peak/trough ratios from 1.3 to 1.6, are not shown. Gstp1 was the most abundantly expressed Gst isoform, which had slightly higher (1.5-fold peak/trough value) mRNA accumulation in the light phase than the dark. Different from the light-phase predominant pattern described above, the theta class of Gsts, Gstt1 and Gstt2, are expressed lowest at 1000. Gstt1 had higher expression at both of the light-dark transition time points (0600 and 1800), and Gstt2 mRNA was expressed more during the dark phase.

Peak/trough ratios were 1.7 fold for both Gstts. The abundantly expressed mRNA of the microsomal Gst isoform mGst1 oscillated with a 1.9-fold magnitude, with peak and trough appearing at 2200 and 1000, respectively. The catalytic subunit of glutamate-cysteine ligase (Gclc) is the rate-limiting enzyme for glutathione synthesis. Gclc expression exhibited circadian variation with the peak appearing at 1000 and trough between 1800 and 2200, with a peak/trough ratio of 2.3.

***Diurnal expression of hepatic efflux transporters*.** The mRNA expression of major drug transporters on the canalicular membrane of hepatocytes oscillated less than 2 fold (Fig. 10), including the efflux transporters Bcrp (1.8 fold), Mrp2 (1.7 fold), Mdr2 (1.5 fold), and Mate1 (1.3 fold), as well as the aminophospholipid flipase Atp8b1 (1.6 fold). However, Mdr1 is the exception that exhibited a 2.9-fold fluctuation, with maximal expression at 2200. The expression of transporters on the sinusoidal membrane of hepatocytes, namely Mrp3, Mrp4, and Mrp6, did not exhibit diurnal fluctuations (peak/trough values between 1.2 and 1.5 fold, data not shown).

***Temporal expression profiles of hepatic transcription factors*.** The majority of hepatic transcription factors examined exhibited peak mRNA expression around the light/dark transition (1400-2200) (Fig. 11). The xenobiotic sensors, PXR and CAR, both peaked at 1800, with 3.2- and 1.7-fold amplitudes, respectively. PPARα and the common nuclear receptor heterodimer partner RXRα reached a ~2.5-fold peak at 1400. Similar to PXR and CAR, AhR and its nuclear heterodimer partner, aryl hydrocarbon receptor nuclear translocator

(Arnt), both demonstrated peak mRNA levels at 1800, with 1.9- and 1.4-fold peak/trough ratios, respectively. Nrf2 expression was consistent across the 24-h time course, except a 50% increase at 1400, whereas the expression of its cytoplasmic repressor Keap1 was higher (40%) during the dark than light phase.

Furthermore, expression of several liver-enriched transcription factors also exhibited dramatic circadian rhythms in mouse liver (Fig. 11). HNF1α mRNA expression did not increase until the onset of the dark phase, whereby a 3-fold peak expression was reached at 2200. HNF4α mRNA increased to the maximum at 1800, with a 2-fold peak/trough ratio. C/EBPα expression exhibited a 1.6-fold peak before the onset of the dark phase at 1400, whereas C/EBPβ mRNA steadily increased to a 2.9-fold peak at 1800, and then gradually decreased during the dark phase.

***Hierarchical cluster analysis of the circadian expression profiles of hepatic DPGs and transcription factors*.** The expression profiles of each DPG and transcription factor across time was analyzed by hierarchical cluster analysis, whereby peak mRNA expression (by time) corresponds with the darkest shaded region of the heatmap (Fig. 12). The circadian expression of hepatic DPGs can be broadly classified into dark-peak or light-peak groups. Interestingly, genes exhibiting peaks during the dark phase (1800, 2200, 0200) include almost all phase-I enzymes, but only a few phase-II enzymes (Sult1d1, Papss2, MGst1, Ugt2b1) and transporters (Mdr1, Bcrp). Conversely, the majority of phase-II conjugation enzymes and transporters exhibit highest mRNA expression in the light phase (0600, 1000, 1400). Transcription factors can be classified into three

major clusters (Fig. 13): the 2200-peak cluster, led by the core clock component Bmal1, comprises transcription factors HNF1α and Keap1; the 1400-peak cluster, led by Rev-Erbα, includes PPARα, Nrf2, C/EBPα, and RXRα; and the 1800-peak cluster, led by DBP, consists of CAR, PXR, HNF4α, AhR, Arnt, and C/EBPβ.

Discussion

Circadian variations in the absorption, distribution, metabolism, and excretion of drugs may influence drug efficacy in the clinical treatment of cancer, cardiovascular disease, bacterial infection, inflammation, etc. (Baraldo, 2008). Comprehensive analysis of circadian expression of hepatic DPGs in this report demonstrates a systemic and progressive temporal detoxification network in the liver.

The present study presents time-dependent variations in mRNA expression of phase-I enzymes participating in reduction (Nqo1), hydrolysis (Cess and Pons), and oxidation (Cyps and Aldhs) of xenobiotics. Higher P450 enzyme activities during the dark phase was previously observed in mouse livers (Radzialowski and Bousquet, 1968). Accordingly, mRNAs of several critical P450 enzymes are more highly expressed at night (Fig.3). Previous reports on the circadian rhythms of Cyp2b10 (Gachon et al., 2006), Cyp2e1 (Matsunaga et al., 2008), and Cyp3a11 (Takiguchi et al., 2007) in mice are comparable to those in this study. In the dark phase, mouse liver robustly expresses Cpr and Alas1 to correspondingly supply Cyps with electrons and heme, respectively. Based on these gene expression profiles, higher Cyp-mediated drug metabolizing ability is expected in the dark phase in the livers of mice.

Temporal mRNA expression profiles of phase-II enzymes in this study support the rhythmic conjugation reactions previously observed in rodents. Glucuronidation is important for xenobiotic biotransformation (Tukey and Strassburg, 2000). Messenger RNA levels of the hepatic Ugts (e.g., Ugt1a1, 1a6,

1a9, 2a3, 2b35, 2b36) are robust in the late-light phase (Fig. 7 and 12), suggesting Ugt enzymes are increased during fasting. Expression of UDP-gpp oscillates in phase with the expression of Ugt enzymes to ensure the availability of the co-substrate UDP-GA. The hepatic concentration of UDP-GA is highest during the fasting period and lowest during the feeding period (Howell and Klaassen, 1991). Similarly, reduced glutathione, the co-substrate for glutathione conjugation, also exhibits a circadian rhythm in liver, with maximum concentration at 1000 and minimal at 1800 (Schnell et al., 1984). Gclc and many Gsts (e.g. Gsta1/2, 1a4, m2, and p1) are maximally expressed during the early-light phase (Fig. 9 and 12). Sulfation in mice is limited by sulfotransferase activity (Liu and Klaassen, 1996). The current study demonstrates that the male predominant Sults (Sult1a1, 1d1, 5a1) (Alnouti and Klaassen, 2006) and the PAPS biosynthesis enzyme PAPSs2 have the highest mRNA expression during the light-to-dark transition. Taken together, phase-II conjugation of xenobiotics in liver may have a circadian rhythm, with more glutathione conjugation in the early-light phase, glucuronidation in the late-light phase, and sulfation in the early-dark phase.

The circadian expression pattern of hepatic enzymes explains at least in part why the hepatotoxicity of xenobiotics, such as acetaminophen, exhibits a circadian rhythm. Kim and Lee showed a single dose of acetaminophen at 2000 produced marked hepatotoxicity in mice, but almost no hepatotoxicity when given at 0800 or 1400 (Kim and Lee, 1998). Glucuronidation or sulfation enzyme activities in liver and concentrations of acetaminophen conjugates in plasma are

similar when acetaminophen was administrated at the three times. However, higher glutathione concentrations were observed at 0800 and lower Cyp enzyme activity occurred at 1400. Therefore, it appears that lower biotransformation by Cyps and higher hepatic glutathione levels, rather than Ugt- or Sult-mediated conjugation, protects livers from acetaminophen-induced liver injury. This speculation is further supported by the current study, where higher expression of Cyps was observed at night (Fig. 3), which corresponds to more hepatotoxicity produced by acetaminophen at 2000, whereas high expression of Gclc in the morning leads to higher hepatic glutathione levels, which provides protection from acetaminophen hepatotoxicity at 0800 (Fig. 9).

Hepatic membrane transporters are involved in the absorption, distribution, and elimination processes of drugs and xenobiotics. However, the circadian rhythms of transporters are not well studied. The mRNAs of sinusoidal uptake transporters, represented by Oatps, coordinately increase prior to the day-to-night transition (Fig. 2), which suggests an anticipation of active hepatic absorption from the portal blood. Via hydrolysis of ATP, the ATP-binding cassette family of transporters actively excrete chemicals from the hepatocytes into bile or blood. Marked circadian rhythm is observed in the mRNA expression of canalicular transporters Mdr1 and Bsep (data not shown), but less oscillations in the mRNA of other canalicular or sinusoidal efflux transporters (Fig. 10). Diurnal variations of Mdr1, Mdr2, and Mrp2 in the present study are consistent with a previous report (Ando et al., 2005). However, Mdr2 mRNA circadian profile differs from another study (Kotaka et al., 2008). Rhythmic variations in the

basal expression of membrane transporters may be important for the diurnal transport of nutrients, metabolic substances, or food-derived toxins in hepatocytes.

Collaboration of enzymes and transporters is an important consideration for hepatic detoxification processes. For instance, in human hepatocytes, the oxidized products by CYPs and the hydrolyzed products by CESs can be further conjugated by UGTs co-localized in the endoplasmic reticulum lumen; the organic anion products by CES-catalyzed hydrolysis and phase-II conjugates are substrates for membrane transporters like MRP2 or BCRP (Hosokawa et al., 2007). DPGs involved in a certain pathway can be simultaneously or sequentially expressed. As demonstrated in hierarchical analysis (Fig. 12), the mRNA expression of phase-I enzymes is abundant in the dark phase, whereas the majority of phase-II enzymes and transporters tend to be robustly expressed towards the end of the light phase. However, most DPGs are highest expressed at 1800, the time to start feeding in mice. Collectively, the rhythmic expression of hepatic DPGs may underly the time-dependent detoxifying capability of the liver.

Hierarchical analysis also reveals that hepatic transcription factors are expressed in-phase with both clock components and DPGs (Fig. 12 and Fig. 13). Thus, the hepatic transcription factors may couple the circadian clock and the daily detoxifying function of the liver. For example, the circadian rhythm of cholesterol 7α-hydroxylase is regulated not only by circadian transcription factors, but also by common nuclear receptors like LXRα, PPARα, and HNF4α (Noshiro et al., 2007). Furthermore, the expression of nuclear receptors might be

subjected to the regulation of the circadian clock. For instance, the circadian expression of CAR and its target gene Cyp2b10 in mouse liver is determined by PARbZip transcription factors (Gachon et al., 2006). Moreover, in rat liver, the phenobarbital-dependent induction of CYP2B1/2 mRNA displays diurnal differences due to the circadian expression of its major regulator CAR (Kanno et al., 2004).

The current study shows that several liver-enriched transcription factors, namely HNF-1α, -4α, C/EBPα and β, have a clear circadian mRNA pattern. The circadian rhythms of these transcription factors are noteworthy because they are thought to regulate the expression of a number of DPGs. For example, mRNA expression of many enzymes and transporters is markedly reduced (Cyp1a2, Cyp2e1, Oat2, Oatp1a1, and 1b2) or increased (Cyp4a14, 7a1, Oct2, Mrp4, Mdr1a, and Mdr2) in HNF-1α-null mouse livers (Maher et al., 2006).

Of note, the circadian clock can directly regulate DPG expression. In a recent study, the knockout of clock-controlled transcription factors including DBP changed the expression of many hepatic DPGs involved in phase-I (Cyp2b, 2c, Ces3, Cpr), phase-II (Gstt1, a3), and transport (Abcg2) processes (Gachon et al., 2006). Collectively, xenobiotic-responsive and circadian transcription factors may together regulate the circadian expression of hepatic DPGs in response to fasting-to-feeding or light-to-dark transitions.

Xenobiotic-activated transcription factors can also affect the clock system. For example, the AhR ligand, 2,3,7,8-tetrachlorodibenzo-*p*-dioxin, is able to alter the expression of Per1 and Bmal1 and decrease phase shifts in response to light

(Mukai et al., 2008). In addition, mRNA of AhR and its target gene Cyp1a1 both exhibit 2-fold diurnal fluctuations (Mukai et al., 2008). Another example is PPARα, which is not only regulated by CLOCK (Oishi et al., 2005), but also regulates Bmal1 expression *in vivo* via direct binding to the Bmal1 promoter (Canaple et al., 2006). Taken together, xenobiotic-activated transcription factors may also exert exogenous influences onto the expression of clock components.

In summary, the current study describes the diurnal expression patterns of important DPGs and transcription factors in mouse liver. Phase-I enzyme mRNA expression is highest during the dark phase, whereas phase-II enzyme and transporter expression is abundant at different times throughout the light phase, thus underlying the temporal variation of drug processing genes in the liver. The in-phase expression of hepatic transcription factors with most of the DPGs and several critical clock components suggests transcription factors are important in coupling the circadian clock and DPG expression. The comprehensive characterization of diurnal patterns of important DPGs and transcription factors provides valuable references for drug development and clinical drug administration.

Acknowledgement

The authors would like to thank Scott Reisman and Dr. Cheryl Rockwell for assistance with the Multiplex Suspension Array, and numerous graduate students and postdoctoral fellows who helped to remove tissues from the mice.

References

Akhtar RA, Reddy AB, Maywood ES, Clayton JD, King VM, Smith AG, Gant TW, Hastings MH and Kyriacou CP (2002) Circadian cycling of the mouse liver transcriptome, as revealed by cDNA microarray, is driven by the suprachiasmatic nucleus. *Curr Biol* **12:**540-550.

Alnouti Y and Klaassen CD (2006) Tissue distribution and ontogeny of sulfotransferase enzymes in mice. *Toxicol. Sci.* **93:**242-255.

Ando H, Yanagihara H, Sugimoto K-i, Hayashi Y, Tsuruoka S, Takamura T, Kaneko S and Fujimura A (2005) Daily rhythms of P-glycoprotein expression in mice. *Chronobiology International* **22:**655 - 665.

Baraldo M (2008) The influence of circadian rhythms on the kinetics of drugs in humans. *Expert Opinion on Drug Metabolism & Toxicology* **4:**175-192.

Canaple L, Rambaud J, Dkhissi-Benyahya O, Rayet B, Tan NS, Michalik L, Delaunay F, Wahli W and Laudet V (2006) Reciprocal regulation of brain and muscle Arnt-like protein 1 and peroxisome proliferator-activated receptor {alpha} defines a novel positive feedback loop in the rodent liver circadian clock. *Mol Endocrinol* **20:**1715-1727.

Cheng X and Klaassen CD (2006) Regulation of mRNA expression of xenobiotic transporters by the pregnane X receptor in mouse liver, kidney, and intestine. *Drug Metab Dispos* **34:**1863-1867.

Cheng X, Maher J, Chen C and Klaassen CD (2005a) Tissue distribution and ontogeny of mouse organic anion transporting polypeptides (OATPs). *Drug Metab Dispos* **33:**1062-1073.

Cheng X, Maher J, Dieter MZ and Klaassen CD (2005b) Regulation of mouse organic anion-transporting polypeptides (OATPs) in liver by prototypical microsomal enzyem inducers that activate distinct transcription factor pathways. *Drug Metab. Dispos.* **33:**1276-1282.

Duffield GE (2003) DNA microarray analyses of circadian timing: the genomic basis of biological time. *J Neuroendocrinol* **15:**991-1002.

Gachon F, Olela FF, Schaad O, Descombes P and Schibler U (2006) The circadian PAR-domain basic leucine zipper transcription factors DBP, TEF, and HLF modulate basal and inducible xenobiotic detoxification. *Cell Metab* **4:**25-36.

Hartley DP and Klaassen CD (2000) Detection of chemical-induced differential expression of rat hepatic cytochrome P450 mRNA transcripts using branched DNA signal amplification technology. *Drug Metab Dispos* **28:**608-616.

Haus E and Smolensky M (2006) Biological Clocks and Shift Work: Circadian Dysregulation and Potential Long-term Effects. *Cancer Causes and Control* **17:**489-500.

Hosokawa M, Furihata T, Yaginuma Y, Yamamoto N, Koyano N, Fujii A, Nagahara Y, Satoh T and Chiba K (2007) Genomic structure and transcriptional regulation of the rat, mouse, and human carboxylesterase genes. *Drug Metab Rev* **39:**1-15.

Howell SR and Klaassen C (1991) Circadian variation of hepatic UDP-glucuronic acid and the glucuronidation of xenobiotics in mice. *Toxicol Lett* **57:**73-79.

Kanno Y, Otsuka S, Hiromasa T, Nakahama T and Inouye Y (2004) Diurnal difference in CAR mRNA expression. *Nuclear Receptor* **2:**6.

Kim YC and Lee SJ (1998) Temporal variation in hepatotoxicity and metabolism of acetaminophen in mice. *Toxicology* **128:**53-61.

Klaassen CD and Lu H (2008) Xenobiotic transporters: ascribing function from gene knockout and mutation studies. *Toxicol Sci* **101:**186-196.

Klaassen CD and Slitt AL (2005) Regulation of hepatic transporters by xenobiotic receptors. *Curr Drug Metab* **6:**309-328.

Kotaka M, Onishi Y, Ohno T, Akaike T and Ishida N (2008) Identification of negative transcriptional factor E4BP4-binding site in the mouse circadian-regulated gene Mdr2. *Neuroscience Research* **60:**307-313.

Levi F and Schibler U (2007) Circadian rhythms: mechanisms and therapeutic implications. *Annu Rev Pharmacol Toxicol* **47:**593-628.

Liu L and Klaassen CD (1996) Different mechanism of saturation of acetaminophen sulfate conjugation in mice and rats. *Toxicology and Applied Pharmacology* **139:**128-134.

Lowrey PL and Takahashi JS (2004) Mammalian circadian biology: elucidating genome-wide levels of temporal organization. *Annu Rev Genomics Hum Genet* **5:**407-441.

Maher JM, Slitt AL, Callaghan TN, Cheng X, Cheung C, Gonzalez FJ and Klaassen CD (2006) Alterations in transporter expression in liver, kidney, and duodenum after targeted disruption of the transcription factor HNF1alpha. *Biochem Pharmacol* **72:**512-522.

Matsunaga N, Ikeda M, Takiguchi T, Koyanagi S and Ohdo S (2008) The molecular mechanism regulating 24-hour rhythm of CYP2E1 expression in the mouse liver. *Hepatology* **48:**240-251.

Mukai M, Lin T-M, Peterson RE, Cooke PS and Tischkau SA (2008) Behavioral rhythmicity of mice lacking AhR and attenuation of light-induced phase shift by 2,3,7,8-tetrachlorodibenzo-p-dioxin. *J Biol Rhythms* **23:**200-210.

Nakata K, Tanaka Y, Nakano T, Adachi T, Tanaka H, Kaminuma T and Ishikawa T (2006) Nuclear receptor-mediated transcriptional regulation in Phase I, II, and III xenobiotic metabolizing systems. *Drug Metab Pharmacokinet* **21:**437-457.

Noshiro M, Usui E, Kawamoto T, Kubo H, Fujimoto K, Furukawa M, Honma S, Makishima M, Honma KI and Kato Y (2007) Multiple mechanisms regulate circadian expression of the gene for cholesterol 7α-hydroxylase (Cyp7a), a key enzyme in hepatic bile acid biosynthesis. *Journal of Biological Rhythms* **22:**299-311.

Oishi K, Shirai H and Ishida N (2005) CLOCK is involved in the circadian transactivation of peroxisome-proliferator-activated receptor alpha (PPARalpha) in mice. *Biochem. J.* **386:**575-581.

Panda S, Antoch MP, Miller BH, Su AI, Schook AB, Straume M, Schultz PG, Kay SA, Takahashi JS and Hogenesch JB (2002) Coordinated transcription of key pathways in the mouse by the circadian clock. *Cell* **109:**307-320.

Parkinson A and Ogilvie BW (2008) Biotransformation of Xenobiotics, in: *Casarett and Doull's Toxicology: the Basic Science of Poisons* (Klaassen CD ed), pp 161-304, McGraw-Hill, New York.

Petrick JS and Klaassen CD (2007) Importance of hepatic induction of constitutive androstane receptor and other transcription factors that regulate xenobiotic metabolism and transport. *Drug Metab Dispos* **35:**1806-1815.

Radzialowski FM and Bousquet WF (1968) Daily rhythmic variation in hepatic drug metabolism in the rat and mouse. *J Pharmacol Exp Ther* **163:**229-238.

Schnell RC, Bozigian HP, Davies MH, Merrick BA, Park KS and McMillan DA (1984) Factors influencing circadian rhythms in acetaminophen lethality. *Pharmacology* **29:**149-157.

Takiguchi T, Tomita M, Matsunaga N, Nakagawa H, Koyanagi S and Ohdo S (2007) Molecular basis for rhythmic expression of CYP3A4 in serum-shocked HepG2 cells. *Pharmacogenet Genomics* **17:**1047-1056.

Tukey RH and Strassburg CP (2000) Human UDP-glucuronosyltransferases: metabolism, expression, and disease. *Annu Rev Pharmacol Toxicol* **40:**581-616.

Footnote

[i] This study is supported by the following grants: ES09649, ES09716, ES 07079, and RR021940.

DMD Fast Forward. Published on October 6, 2008 as DOI: 10.1124/dmd.108.024174
This article has not been copyedited and formatted. The final version may differ from this version.

Figure Legends

Fig. 1. Rhythmic transcripts of protypical circadian oscillators (Bmal1 and Rev-Erbα) and clock-controlled gene (Dbp) in mouse liver. Total RNA from mouse livers (n=5 per time point) was pooled and mRNA expression was determined by multiplex suspension array. Data at 0600 were used twice to graph a 24-h cycle of mRNA expression. Numbers in the parentheses next to gene names indicate peak/trough ratio of each mRNA. Shaded area of the figure represents dark phase and white area for the light phase. The same design is also used in the following figures.

Fig. 2. Daily mRNA expression profiles of basolateral uptake transporters in mouse liver. Graphical presentation follows that outlined in Figure 1.

Fig. 3. Daily mRNA expression profiles of major cytochrome P450 (Cyp) enzymes in mouse liver. Graphical presentation follows that outlined in Figure 1. *Branched DNA assay was employed to determine the mRNA expression Cyp2e1 and 3a11 with 1 μg pooled RNA (n=5 per time point), and 10 μg for Cyp2b10.

Fig. 4. Daily mRNA expression profiles of representative aldehyde dehydrogenases (Aldhs) in mouse liver. Graphical presentation follows that outlined in Figure 1.

Fig. 5. Daily mRNA expression profiles of representative carboxylesterases (Cess) in mouse liver. Graphical presentation follows that outlined in Figure 1. *Expression profile of Ces5b1 was quantified by bDNA with 1 μg pooled RNA (n=5 per time point).

Fig. 6. Daily mRNA expression profiles of paraoxonases (Pons) and NAD(P)H-quinone oxidoreductase 1 (Nqo1) in mouse liver. Graphical presentation follows that outlined in Figure 1. *Expression profile of Pon1 was quantified by bDNA with 1 μg RNA from 5 mouse livers per time point.

Fig. 7. Representative circadian expression profiles of hepatic UDP-glucuronosyltransferase (Ugt) isoforms and UDP-GA biosynthesis enzymes. Graphical presentation follows that outlined in Figure 1.

Fig. 8. Representative rhythmic expression patterns of hepatic sulfotransferase (Sult) isoforms and PAPS synthase. Graphical presentation follows that outlined in Figure 1.

Fig. 9. Representative circadian expression profiles hepatic glutathione *S*-transferase (Gst) isoforms and glutamate-cysteine ligase catalytic subunit (Gclc). Graphical presentation follows that outlined in Figure 1.

Fig. 10. Daily mRNA expression profiles of canalicular transporters in mouse liver. Graphical presentation follows that outlined in Figure 1. *Expression of Mdr1 mRNA was quantified by bDNA assay with 10 µg pooled RNA (n=5 per time point).

Fig. 11. Diurnal expression profiles of important xenobiotic-metabolism transcription factors in the liver. Graphical presentation follows that outlined in Figure 1. *Messenger RNA expression of Keap1 and AhR was quantified by bDNA assay with 10 µg pooled RNA (n=5 per time point).

Fig. 12. Hierarchical cluster analysis of temporal expression profiles of major drug processing genes. Each column represents a circadian time point and each row a gene with the name indicated beside. The number in parenthesis, beside each gene name, represents mRNA expression peak/trough ratio of that particular gene. Numbers at the top depict the time of day, and the bar represents the light phase (white) or dark phase (black). Peak expression for each gene is represented by the darkest region of the gray-scale spectrum, and lowest expression indicated by the lightest (gray) region. Each spectrum is specific to the scale of mRNA expression for each gene on an individual basis. Therefore, comparing gene expression profiles across gray-scale spectra is not valid due to differences in relative gene expression.

Fig. 13. Hierarchical cluster analysis of the diurnal expression of hepatic transcription factors. Graphical presentation follows that outlined in Figure 12.

Fig. 1

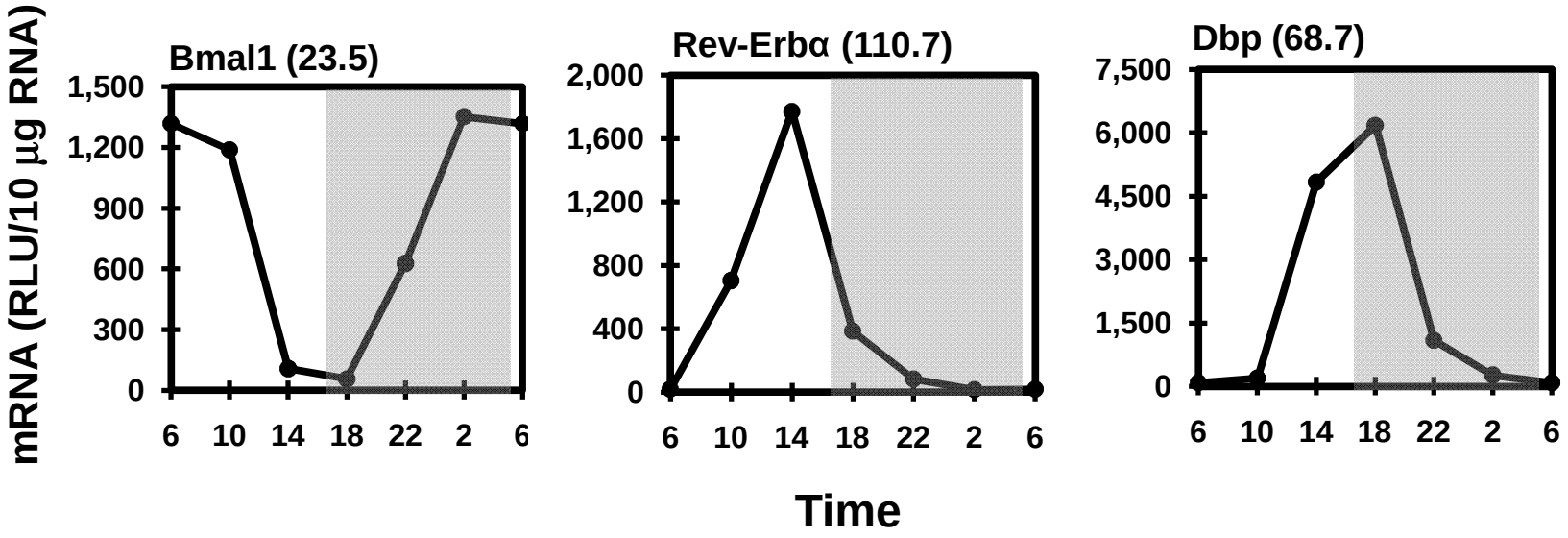

Fig. 2

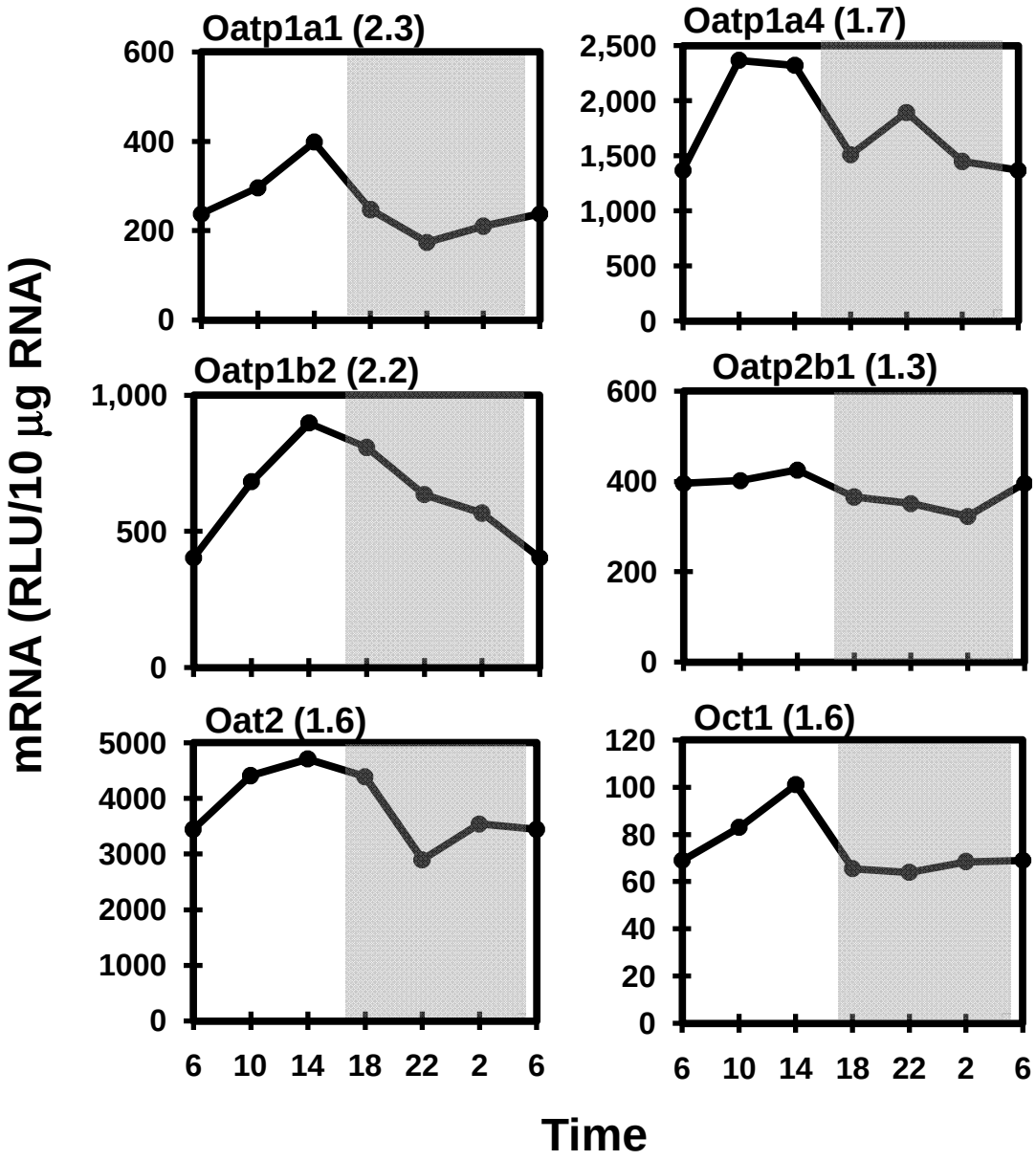

Fig. 3

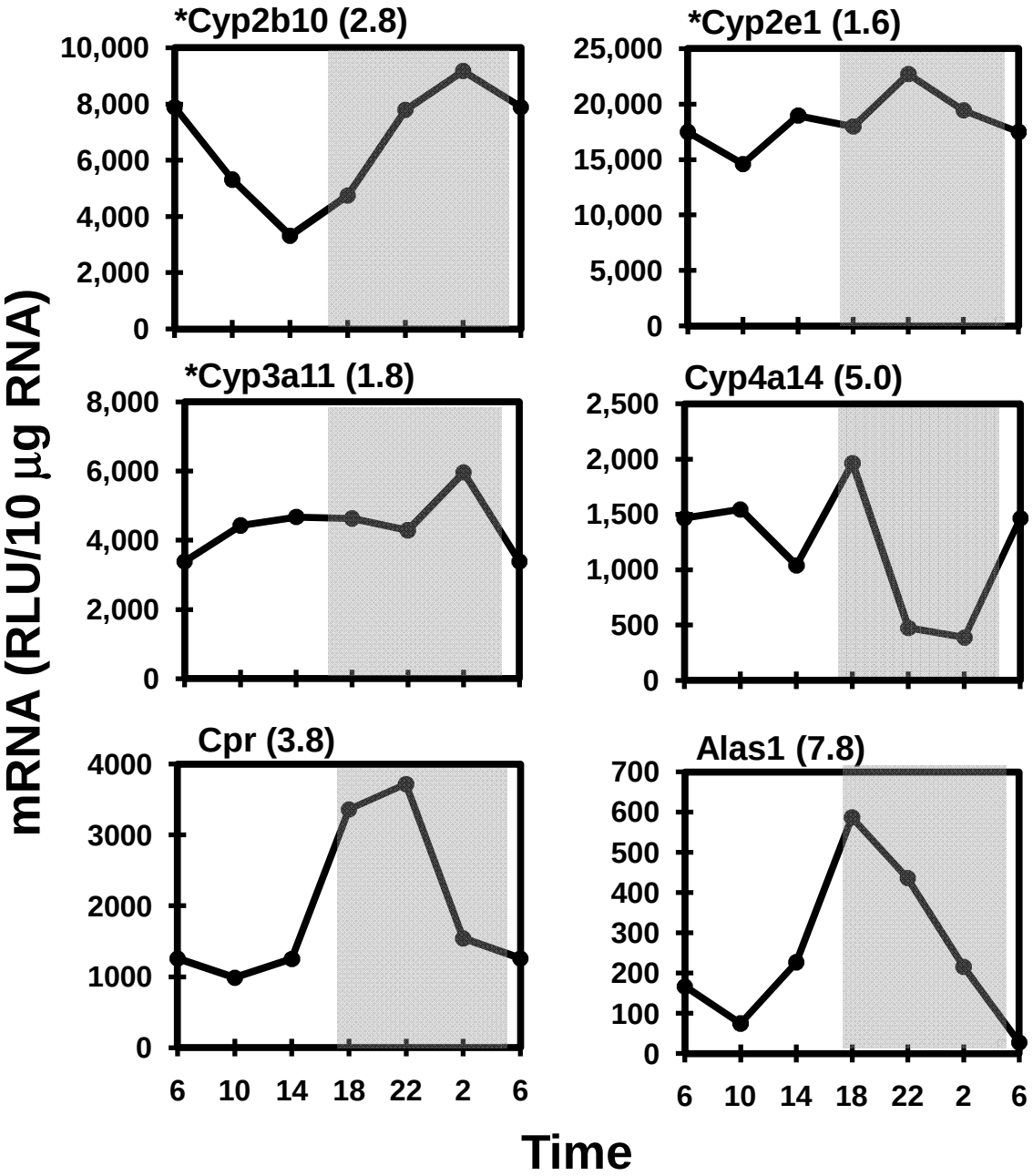

Fig. 4

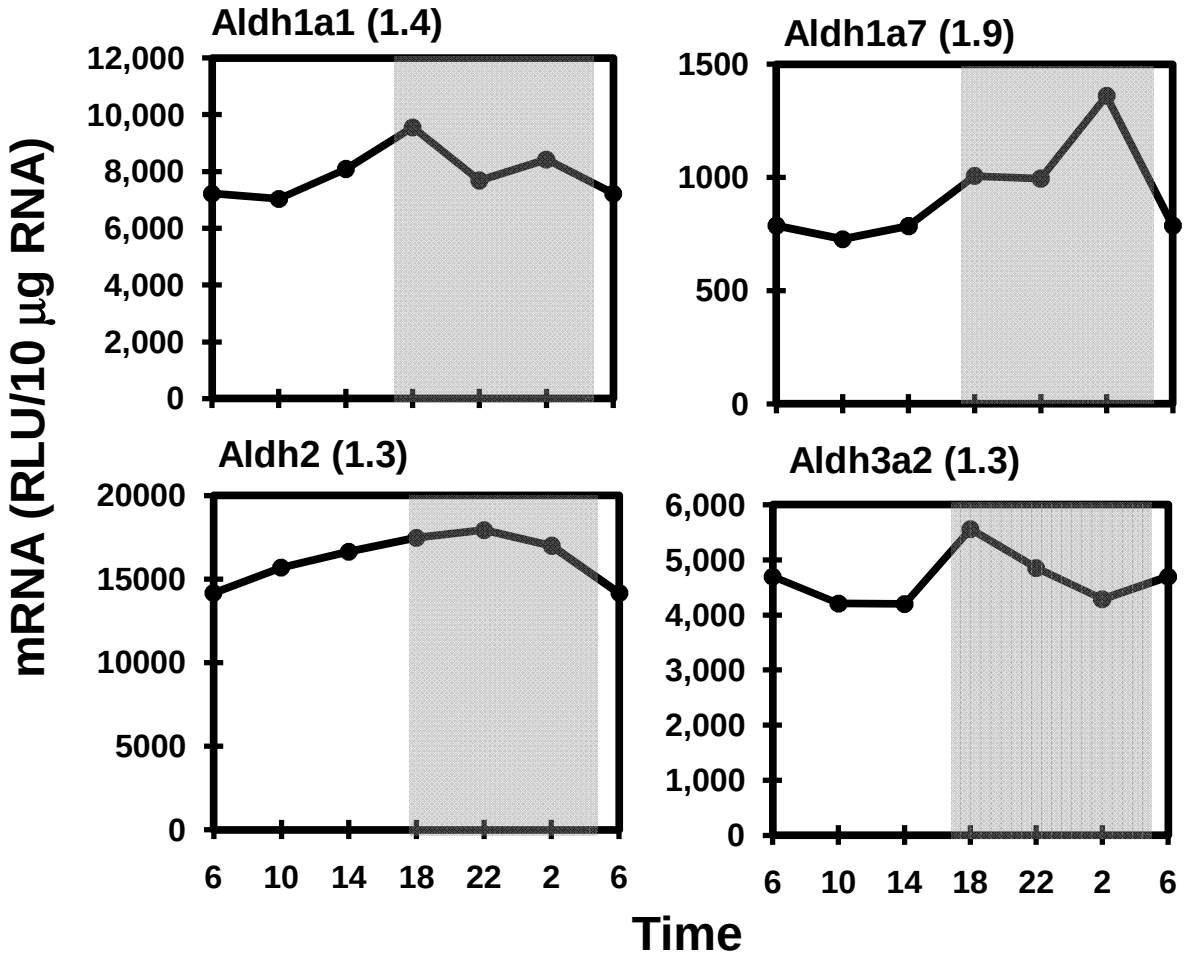

Fig. 5

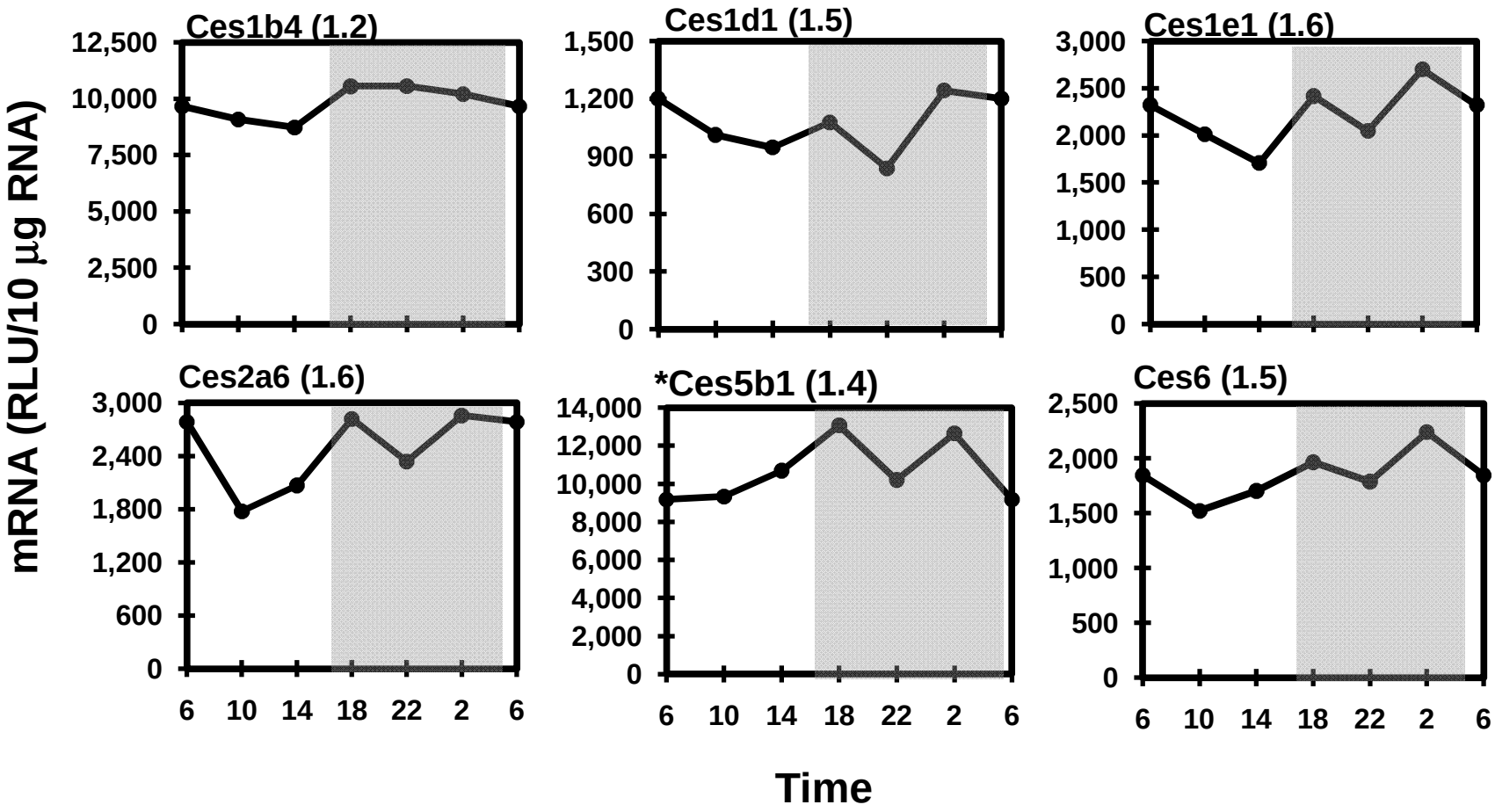

Fig. 6

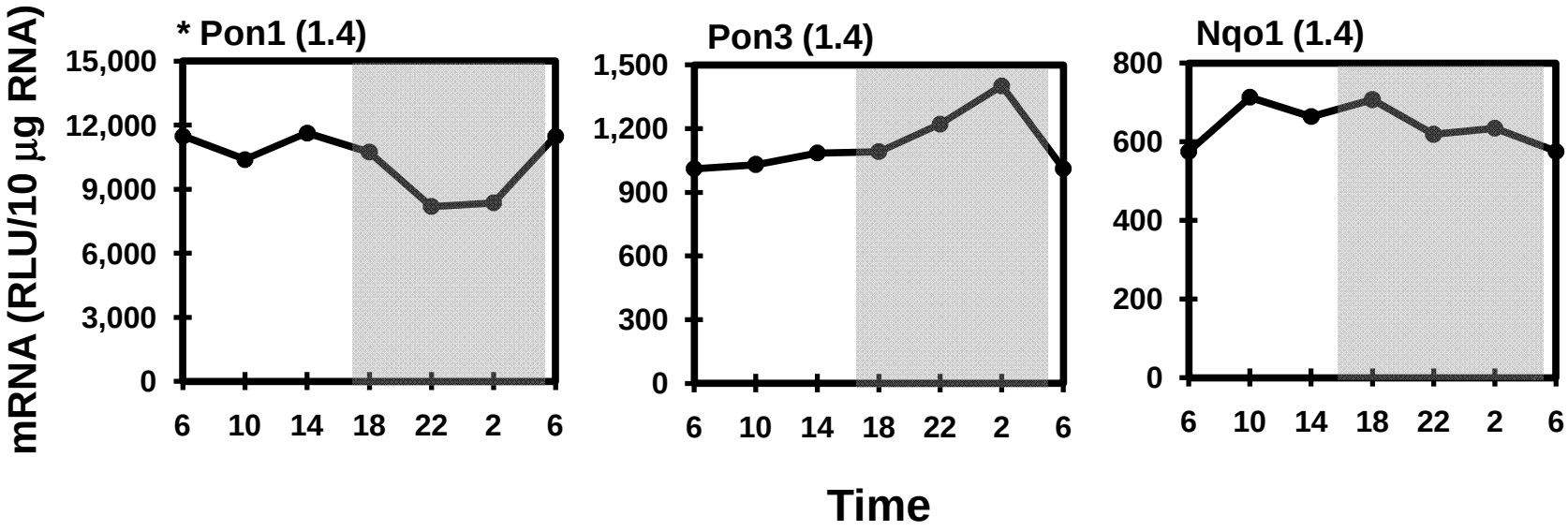

Fig. 7

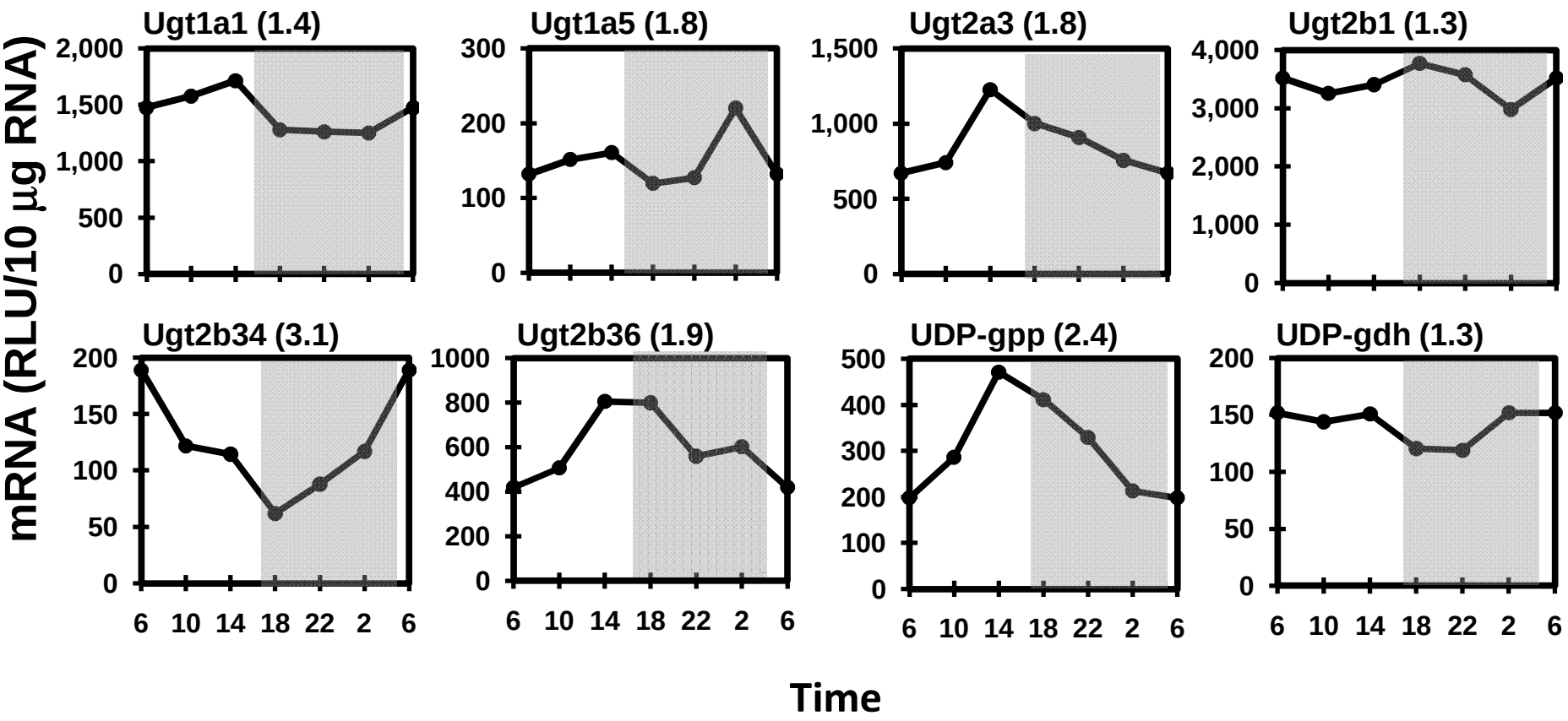

Fig. 8

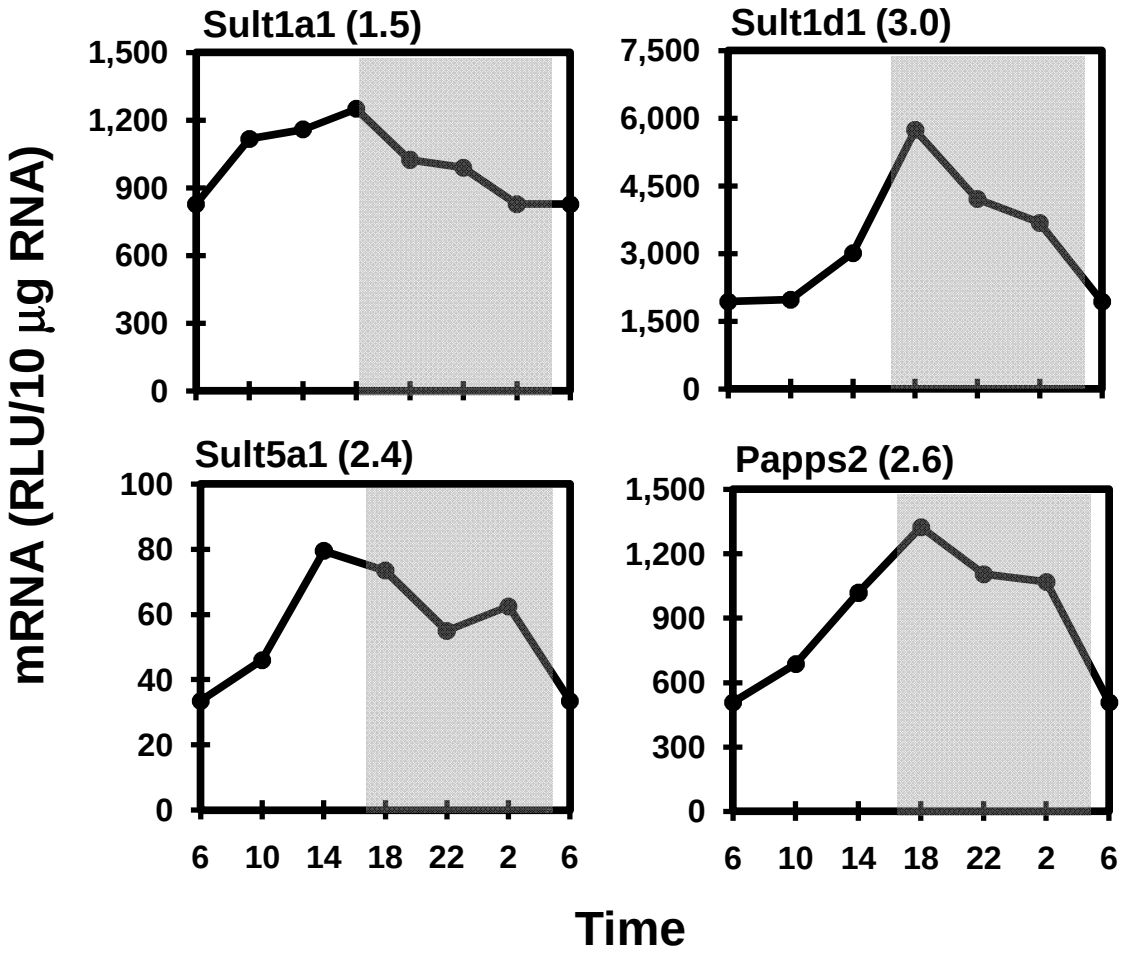

Fig. 9

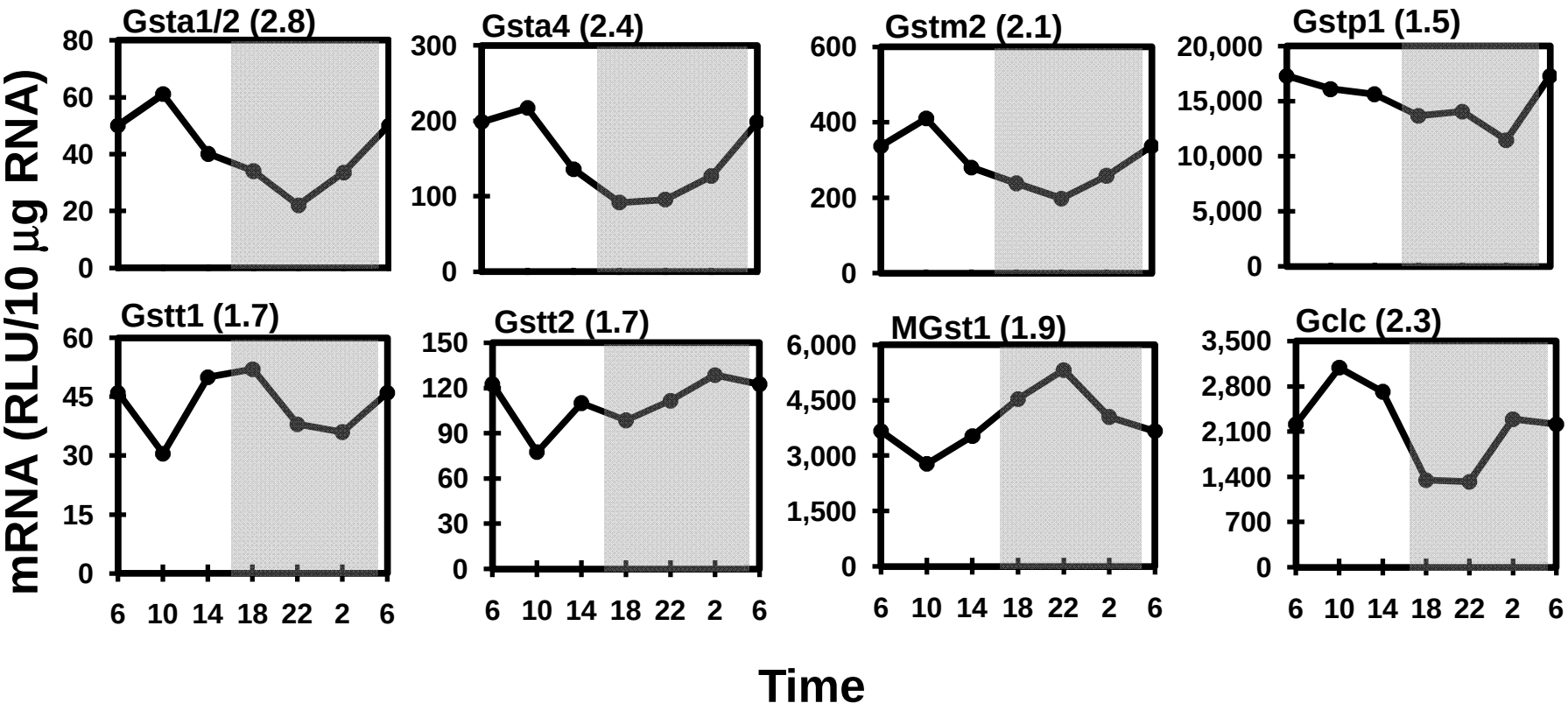

Fig. 10

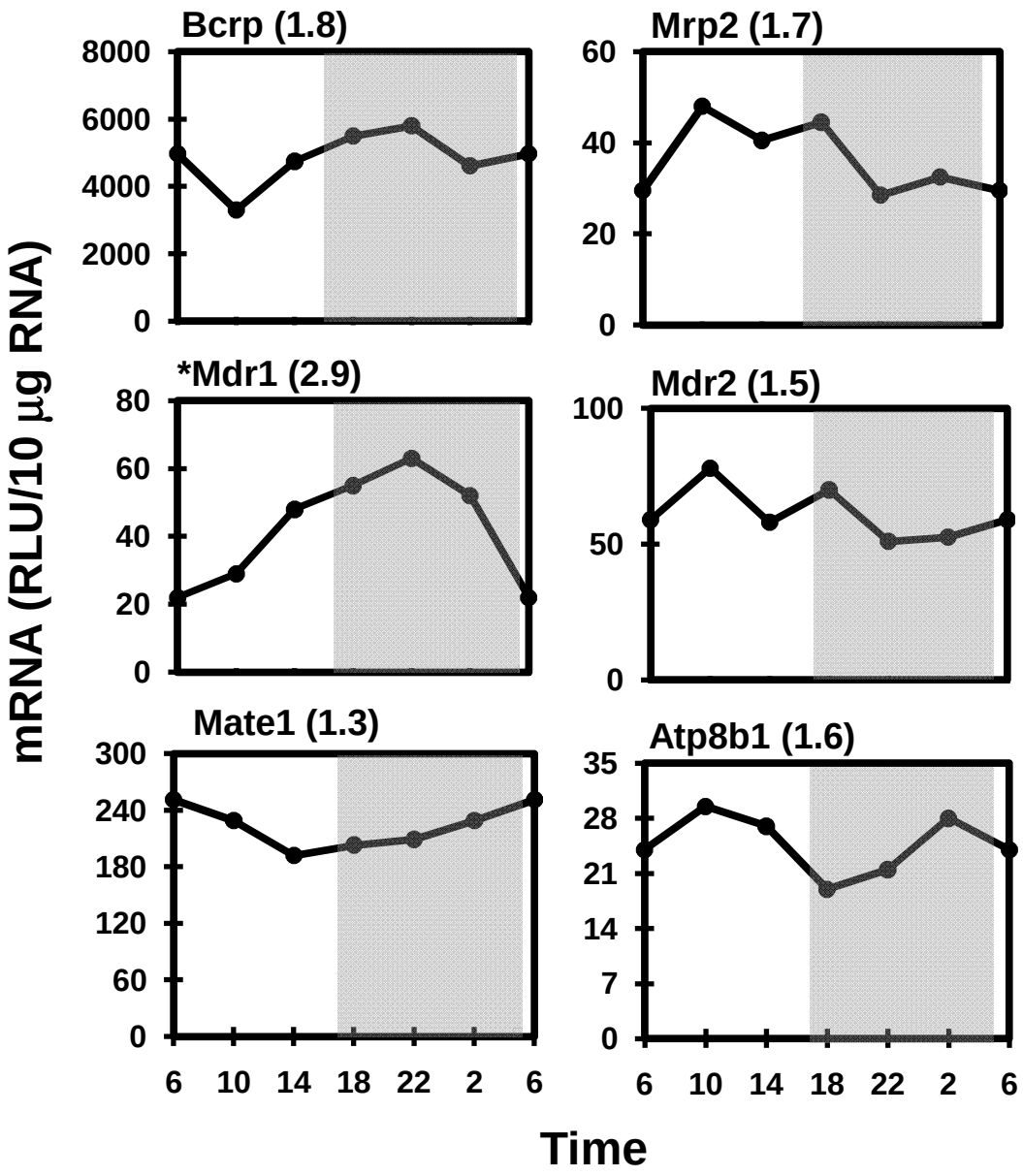

Fig. 11

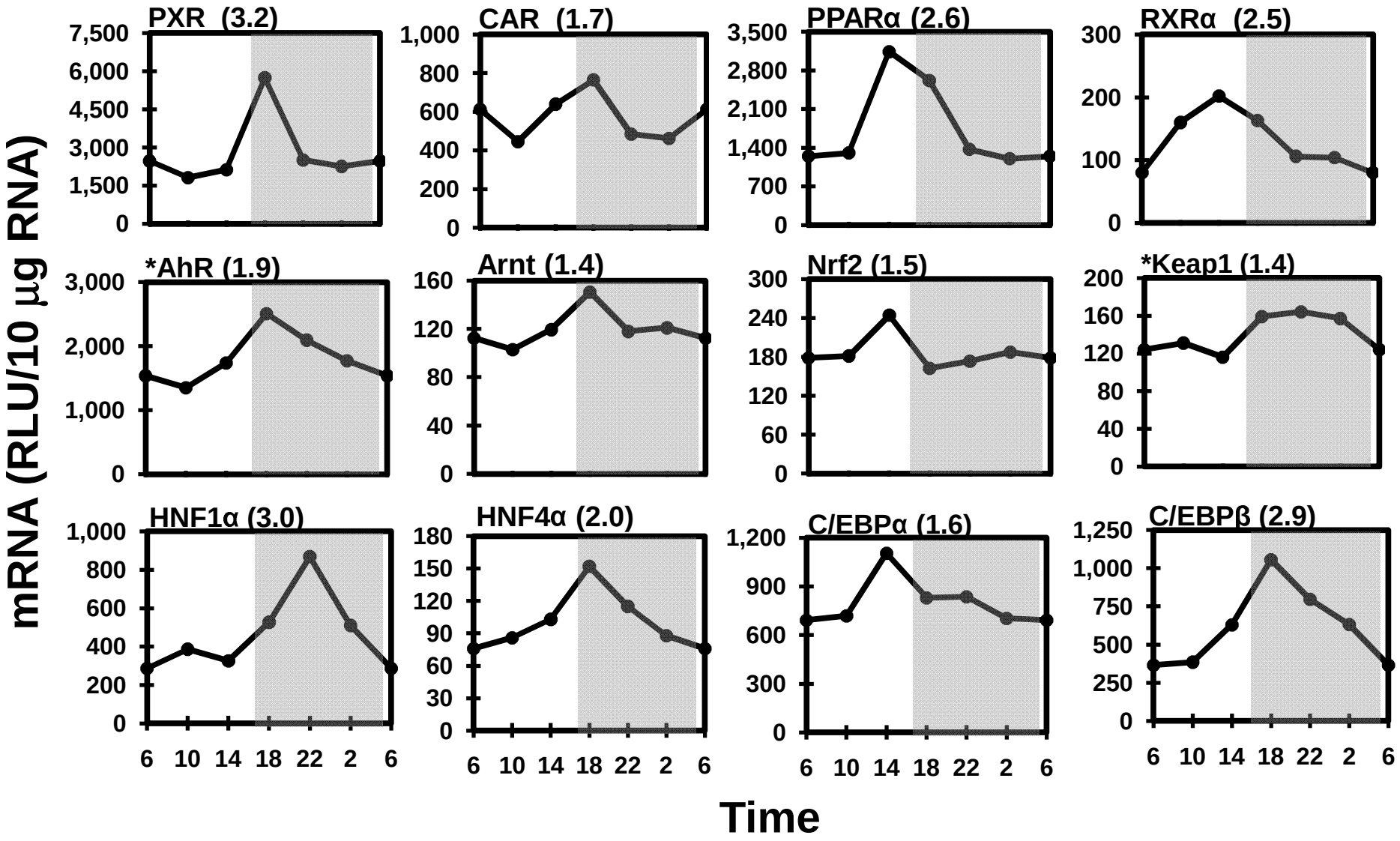

Fig. 12

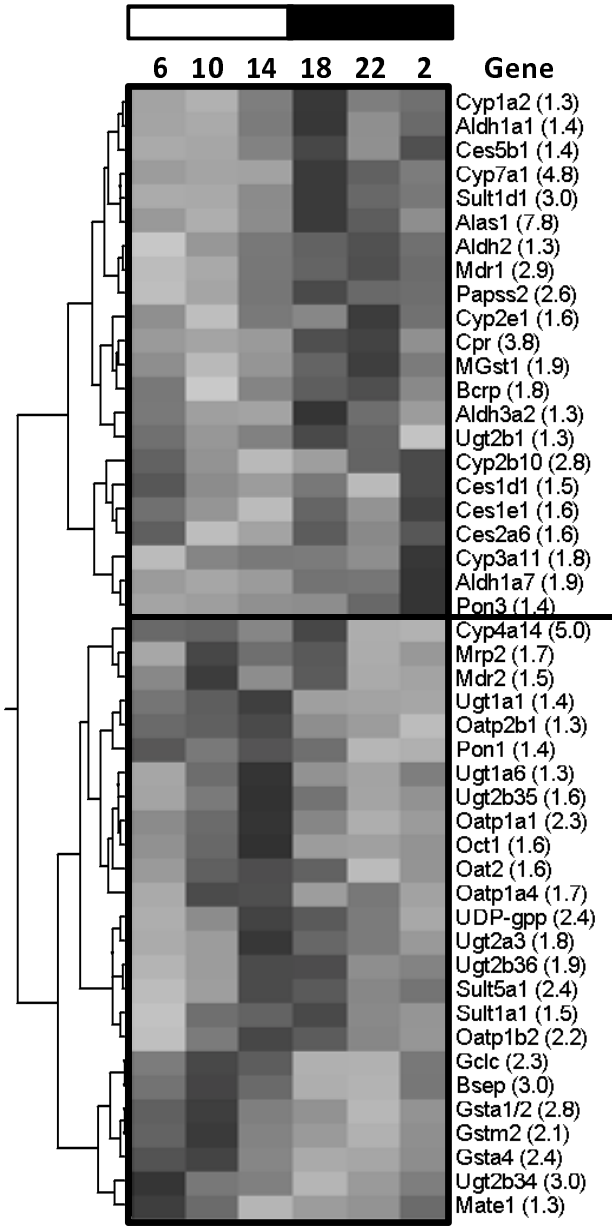

Fig. 13